Journal of Architectural Research and Development, 2023, Volume 7, Issue 2
http://ojs.bbwpublisher.com/index.php/JARD
ISSN Online: 2208-3537
ISSN Print: 2208-3529

Load Test Analysis and Research on Long-Span Concrete Continuous Rigid Frame Bridge

Lin Nan, Yan Liu*, Guangjun Li, Yingying Ye, Shuguo Wang, Qiang Yang

China Merchants Chongqing Highway Engineering Testing Center Co., Ltd., Chongqing 400060, China

***Corresponding author:** Yan Liu, 17880032@qq.com

Abstract: Based on the as-built load test of a large bridge, this paper introduces the procedure of the prestressed concrete continuous rigid frame bridge load test. Numerical analysis of the bridge was carried out by simulating and establishing a finite element model, and comparative analysis was carried out with the measured values. The results show that the calculated values were basically consistent with the measured values, which showed that the establishment method of the model was reasonable, and the mechanical performance of the bridge met the service requirements of the designed live load.

Keywords: Bridge; Continuous rigid frame; Load test

Online publication: March 30, 2023

1. Introduction

As an artificial structure in the outdoor environment, bridges have a long service time, and they are subjected to harsh environmental conditions and heavy loads. In order to test the bridge design, construction quality, and the reliability of the project, a load test is usually carried out to understand the actual working state of the tested bridge span under the test load. After testing and analysis, the actual bearing capacity of the bridge is determined and its working performance under the designed load is evaluated. Based on the as-built load test of a bridge, the load test of continuous rigid frame bridge was studied in this paper. The test methods and results can be used as a reference for similar bridges [1-3].

2. Project overview

The main part of the bridge was 267 m long, and the bridge span layout and structural form are (68.5 + 130 + 68.5)m three-span continuous rigid frame bridge, which was divided into left and right layouts. Each main girder was a box girder. The steepness of the horizontal slope of the top of the box girder was the same as the road arch, which is 1.5%. The top width of the box girder was 1520 cm, the bottom width was 700 cm, the center height of the root of the box girder was 780 cm, and the height of the midspan beam was 280 cm. The main pier adopted a double-leg thin-walled pier, and the pier body was consolidated with the superstructure box girder. Asphalt concrete bridge deck pavement was used for roadway bridge deck pavement.

Design load = urban-level A + crowd load 3.0 kPa

Bridge design cross-section = 3 m (sidewalk) + 11.5 m (roadway) + 2.0 m (separation zone) + 11.5 m (roadway) + 3 m (sidewalk)
= total width 31 m

3. Test content

In order to determine the number of loading vehicles and the loading position of the load test, the corresponding finite element calculation and analysis of the bridge was carried out. The static load test of the bridge was mainly used to check the extent to which the displacement or stress of the main load-bearing member control section of the bridge span structure was in line with the design expectation under the most unfavorable live load. The test items included stress, displacement, and cracks. The dynamic test was performed to understand natural vibration characteristics of the bridge span structure and the dynamic response under the load, and to analyze its dynamic performance in the long-term. The test items included frequency, damping ratio, and response towards forced vibration under dynamic load, such as dynamic strain and impact coefficient [4-6].

According to the structural characteristics of the test bridge span, three sections were selected as control sections. The position of each control section is shown in **Figure 1**. The test section and measuring point layout of the structural modal parameters are shown in **Figure 2**. The test content is shown in **Table 1**.

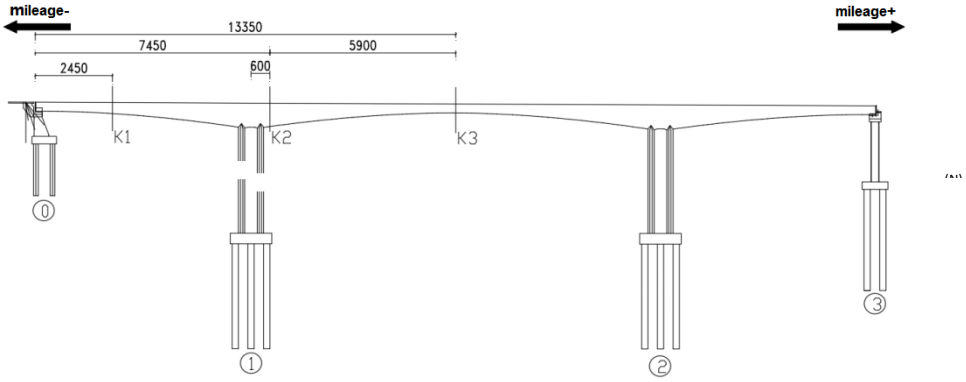

Figure 1. Schematic diagram of control section layout (unit: cm)

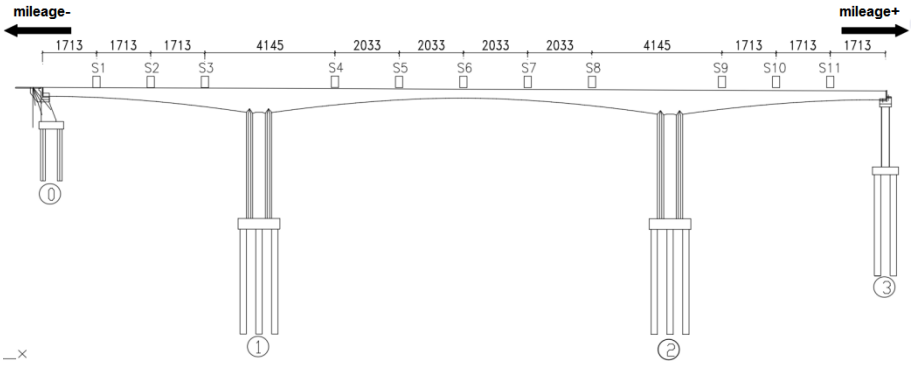

Figure 2. Schematic diagram of the layout of the modal test measuring points (unit: cm)

Table 1. Test control section and test content

Section number	Control section	Test content
K1	The maximum positive bend of the main girder of the first span	Static strain, deflection, crack, dynamic strain
K2	The maximum negative bending of the main girder of No. 1 pier	Static strain, crack
K3	The maximum positive bend of the main girder of the second span	Static strain, deflection, crack, dynamic strain

4. Design of test scheme

4.1. Static load scheme

According to relevant specifications [7], the range of load efficiency in this static load test was $0.85 < \eta \leq 1.05$. A total of 6 loading conditions were designed in this test, numbered J1–J6. The loading vehicle was a 3-axle muck truck, the weight of a single vehicle was controlled at 350 kN ± 10 kN, the (middle) rear axle was controlled at 140 kN, and the front (middle) axle was controlled at 70kN. The maximum number of vehicles used in the test was 9, and the minimum was 6, which meant that the loading efficiency of each working condition met the specifications. The control section and vehicle consumption included in each working condition are shown in **Table 2**, and the control section numbers in the table correspond to **Table 1**.

Table 2. Loading efficiency and vehicle consumption under each working condition

Case number	Loading method	Load feature	Loading efficiency	Vehicle use number
J1	Positive load	Positive bending moment (K1)	0.95	6
J2	To the right	Positive bending moment (K1)	0.95	6
J3	Positive load	Negative bending moment (K2)	0.91	9
J4	To the right	Negative bending moment (K2)	0.91	9
J5	Positive load	Positive bending moment (K3)	0.98	9
J6	To the right	Positive bending moment (K3)	0.98	9

The static load test strain measuring points were located inside the box girder. There were 13 measuring points in total on a single section, including 4 on the top plate, 5 on the bottom plate, and 2 on each of the left and right webs; the points were spread evenly on the bridge surface.

4.2. Dynamic load scheme

According to the relevant specifications and the actual situation of the site, the dynamic characteristic test was carried out by using the earth pulsation excitation method and the barrier-free driving test. In the barrier-free driving condition, a 350kN heavy vehicle was driven along the center line of the roadway. The specific content of the dynamic load test is shown in **Table 3**.

Table 3. Description of dynamic load test working condition

Case number	Working condition
D1	Pulsation
D2	1 vehicle crossing the bridge at a constant speed of 5 km/h on the center line
D3	1 vehicle crossing the bridge at a constant speed of 10 km/h on the center line
D4	1 vehicle crossing bridge at a constant speed of 20 km/h on the center line
D5	1 vehicle crossing the bridge at a constant speed of 30 km/h on the center line
D6	1 vehicle crossing the bridge at a constant speed of 40 km/h on the center line

A total of 11 modal measuring points were placed along the centerline of the bridge deck, and the longitudinal positions are shown in **Figure 3**; the positions and numbers of the dynamic strain measuring points were the same as those in the static load test, and two measuring points in the middle of the bottom plate of each section were selected.

5. Test results

5.1. Static load test results

5.1.1. Strain test results

The strain observation results of each control section under the selected loading conditions J1–J6 are listed in **Table 4**. The elastic strain was the difference between the full load strain and the residual strain, and the theoretical value was the value calculated using the finite element model.

Table 3. Strain test results and calibration coefficients

Loading condition	Location of measuring point	Maximum elastic strain (με)	Theoretical value (με)	Calibration coefficient range	Relative residual range (%)
J1	K1	22	50	0.40–0.57	≤ 9.1
J2	K1	23	53	0.40–0.69	≤ 5.3
J3	K2	24	30	0.38–0.80	≤ 11.1
J4	K2	24	32	0.35–0.79	≤ 6.3
J5	K3	54	80	0.37–0.68	≤ 8.5
J6	K3	52	84	0.39–0.66	≤ 5.6

It can be seen from **Table 4** that the maximum strain values were generally smaller than the theoretical values, the calibration coefficient was between 0.35 and 0.80, and the relative residual was less than 20%, which indicated that the strength of the test bridge span met the design requirements.

5.1.2. Deflection test results

The main control sections of the main girder deflection are K1 and K3, which were realized by loading conditions J1, J2, J5, and J6. The measured results are shown in **Table 5**. The elastic displacement was the difference between the full load displacement and the residual displacement, and the theoretical calculation value was calculated using the finite element model.

Table 5. The deflection observation results and calibration coefficients of the main control section of the main girder

Loading condition	Location of measuring point	Maximum elastic displacement (mm)	Theoretical value (mm)	Calibration coefficient range	Relative residual range (%)
J1	K1	3.7	6.8	0.49–0.54	≤ 9.8
J2	K1	3.9	7.1	0.49–0.55	≤ 5.7
J5	K3	14.4	24.3	0.53–0.59	≤ 4.8
J6	K3	14.0	25.5	0.54–0.57	≤ 2.1

Based on **Table 5,** the deflection of the control section under each working condition was smaller than the theoretical value, the calibration coefficient was between 0.49 and 0.59, and the relative residual was less than 20%, indicating that the stiffness of the bridge met the design requirements.

5.2. Dynamic load test results

5.2.1. Measurement results of modal parameters

The results of the modal parameters are shown in **Table 6**, where the theoretical frequency was calculated by the finite element model.

Table 6. Results of bridge model parameters

Number of executions	Measured frequency (Hz)	Damping ratio (%)	Theoretical frequency (Hz)	Mode shape
1	1.395	0.46	1.272	First-order vertical bending of main beam
2	2.620	0.93	2.476	Second-order vertical bending of main beam
3	3.250	1.92	2.833	Three-order vertical bending of the main beam

As shown in **Table 6**, under the corresponding model shapes, the measured frequency of the structure was greater than the theoretical frequency.

5.2.2. Dynamic response test results

According to relevant regulations [8], when the measured vertical fundamental frequency of the bridge structure is f = 1.2719 Hz, the calculated impact coefficient is μ_c = 0.050. The results of the impact coefficient of the bridge structure are shown in **Table 7**.

Table 7. Results of impact coefficient of bridge structure

Location of measuring point	5 km/h driving speed	10 km/h driving speed	20 km/h driving speed	30 km/h driving speed	40 km/h driving speed
K1	0.072	0.055	0.098	0.075	0.096
K1	0.093	0.049	0.101	0.081	0.103
K3	0.028	0.020	0.022	0.020	0.036
K3	0.037	0.044	0.024	0.023	0.049

Based on **Table 7**, the measured impact coefficient of the K1 section of the main bridge was between 0.049 and 0.103, and the measured impact coefficient of the K3 section was between 0.020 and 0.049. The measured impact coefficient of the K3 section was smaller than the theoretical value, but the measured impact coefficient of the K1 section was slightly larger than the theoretical value. This can be due to the low efficiency of the dynamic load test, which was within the normal range compared with similar bridges.

6. Conclusion

The strain test values and girder displacement in the static load test of the continuous rigid frame bridge were all within a reasonable range, the calculated values were smaller than the theoretical values, and the calibration coefficient and relative residual all met the specifications [9]. In the dynamic load test, the measured values of the first three vertical vibration frequencies of the bridge structure were greater than the theoretical values, and the impact coefficients are all within the normal range.

(1) The mechanical performance of the continuous rigid frame bridge met the normal use requirements of the urban-A level and the crowd load of 3.0 kPa.
(2) The dynamic characteristics and dynamic response performance of the inspected span structure of the continuous rigid frame bridge were normal.
(3) The finite element model was relatively accurate in simulating the actual stress state of the bridge, and the design of this test scheme was reasonable.

Disclosure statement

The authors declare no conflict of interest.

References

[1] Nan L, Bai G, Chen C, et al., 2022, Static Test Analysis of Chongqing Dongshuimen Yangtze River Bridge. Highway Traffic Technology, 38(05): 86–93.

[2] Yi B, Li G, Xie G, et al., 2018, Load Test Research on Cuntan Yangtze River Bridge. Highway Traffic Technology, 34(04): 68–75.

[3] Yi B, Hu J, 2015, Load Test and Bearing Capacity Evaluation of Single-Cable Plane Steel Truss Girder Cable-Stayed Bridge for Highway and Rail. Highway and Auto Transport, 2015(1): 184–189.

[4] Huang J, Liu D, 2022, Analysis of the Influence of Calibration Coefficients of Long-span Continuous Rigid Frame Bridges. Henan Science and Technology, 41(08): 65–68.

[5] Du T, Wang F, 2021, Load Test of a Long-Span Continuous Rigid Frame Bridge. Journal of Hubei Institute of Technology, 37(04): 36–41.

[6] Huang G, 2020, Detection and Analysis of Some Key Parameters in the Identification of Continuous Rigid Frame Bridge Bearing Capacity. Highway Traffic Technology, 36(04): 83–89.

[7] Chang'an University, 2015, Regulations for Load Test of Highway Bridges, JTG/T J21-01-2015, viewed December 20, 2022.

[8] China Communications Highway Planning and Design Institute Co., Ltd., 2015, General Specifications for Design of Highway Bridges and Culverts, JTG D60-2015, viewed December 20, 2022.

[9] Highway Research Institute of the Ministry of Transport 2011, Regulations for Testing and Evaluation of Highway Bridge Bearing Capacity, JTG/T J21-2011, viewed December 20, 2022.